K. Kassapidou
W. Jesse
J. A. P. P. van Dijk
J. R. C. van der Maarel
Leiden Institute of Chemistry,
Gorlaeus Laboratories,
Leiden University,
P. O. Box 9502
2300 RA Leiden,
The Netherlands

Received 19 November 1997;
accepted 27 January 1998

Liquid Crystal Formation in DNA Fragment Solutions

Abstract: *The critical volume fractions pertaining to the formation of DNA liquid crystals were obtained from polarization microscopy, ^{31}P-nmr, and phase separation experiments. The DNA length (approximately one to two times the persistence length 50 nm), ionic strength, and counterion variety dependencies are reported. The cholesteric–isotropic transition is interpreted in terms of the coexistence equations, which are derived from the solution free energy including orientational entropy and excluded volume effects. With the wormlike chain as reference system, the electrostatic contribution to the free energy is evaluated as a thermodynamic perturbation in the second virial approximation with a Debye–Hückel potential of mean force. The hard core contribution has been evaluated with scaled particle theory and/or a simple generalization of the Carnahan–Starling equation of state for hard spheres. For sufficiently high ionic strengths, the agreement is almost quantitative. At lower amounts of added salt deviations are observed, which are tentatively attributed to counterion screening effects. The contour length dependence agrees with a DNA persistence length 50 nm.* © 1998 John Wiley & Sons, Inc. Biopoly 46: 31–37, 1998

Keywords: *DNA liquid crystals; DNA fragments; screened Coulomb interactions*

INTRODUCTION

The ability of DNA to form cholesteric liquid crystals has initially been noticed by Robinson in 1961.[1] DNA liquid crystalline structures have also been observed in plasmid DNA in bacteria, viruses, mitochondria, and in vitro.[2–4] Linear DNA dispersed in water or salt solutions shows at least two first-order transitions from the isotropic, through the cholesteric, to the columnar hexagonal phase, if the DNA volume fraction is increased. Before the appearance of the cholesteric phase, blue phases and/or precholesteric phases have been reported, whereas very concentrated phases are true crystals.[2,4] The phase diagram depends on, e.g., solvent ionic strength, DNA contour length, and counterion species. For a recent review of liquid crystalline condensed DNA phases the reader is referred to Ref. 2.

In another publication, we focus on the melting of the columnar hexagonal phase of short persistence length DNA fragments (with most probable length $L = 42$ nm).[5] Here, we report the DNA

Correspondence to: J. R. C. van der Maarel
Biopolymers, Vol. 46, 31–37 (1998)

CCC 0006-3525/98/010031-07

length, ionic strength, and counterion species dependence of the cholesteric–isotropic (C-I) phase transition. The weight average contour length ranges from 42 to 104 nm, which is approximately one to two times the persistence length. The DNA molecules can be considered as semiflexible wormlike chains, surrounded by a double layer formed by counterions and possibly added salt. The phase boundaries are obtained from steplike dilution experiments of equilibrated liquid crystalline samples under parallel inspection by polarized light microscopy and ^{31}P-NMR.[2,4] The C-I phase boundary concentrations were also determined from phase separation experiments.[6,7] For this purpose, biphasic solutions with approximately equal isotropic and liquid crystalline volume fractions were prepared and within the coexisting phases the DNA concentrations were determined by uv spectroscopy.

The C-I phase boundaries can be compared to theoretical predictions based on the coexistence equations, which are derived from the solution free energy including orientational entropy and (electrostatic) excluded volume effects of semiflexible particles.[8,9] With the wormlike chain as reference system, the electrostatic contribution to the free energy is evaluated as a thermodynamic perturbation in the second virial approximation with a Debye–Hückel potential of mean force. For relatively stiff polyelectrolytes with a large length over breadth aspect ratio, reasonable agreement is observed when the hard core contribution is also evaluated in the second virial approximation.[6,7] However, our DNA fragments are rather short and the virial expansion for the reference system has to be carried to higher order. We will use two approximate methods, which have been devised for hard spherocylinders at higher volume fraction and/or smaller aspect ratio: Cotter's scaled particle theory and a simple generalization of the Carnahan–Starling equation of state for hard spheres.[10,11] Both approaches lack rigorous theoretical justification, but their results improve significantly over the second virial expansion and compare favorably with the present DNA results at sufficiently high salt concentration.[12,13] With low amounts of added salt, deviations are observed, which are tentatively attributed to counterion screening effects.

THEORY

In the Debye–Hückel approximation, for two rodlike polyelectrolytes skewed at an angle ϕ the electrostatic potential has the form[14]

$$\frac{w}{kT} = \frac{Ae^{-\kappa x}}{\sin \phi} \tag{1}$$

where x denotes the shortest distance between the central axes and the constant A depends on the polyion properties. For a discussion of the latter parameter, the reader is referred to Ref. 15. For solutions in excess simple salt with ionic strength I, the screening length κ^{-1} is given by $\kappa^2 = 8\pi QI$ with the Bjerrum length $Q = e^2/\epsilon kT$.

In the second virial approximation (for both electrostatic and hard core interactions), the Helmholtz free energy of a solution of N rodlike polyelectrolytes is given by[15]

$$\frac{\Delta F}{N\,kT} = \text{constant} + \ln c_p + \sigma_E - \frac{1}{2} c_p \langle \beta \rangle \tag{2}$$

with σ_E the orientation entropy and c_p the rod number concentration N/V. For hard spherocylinders with length L and bare diameter D_0, Sato and Teramoto have derived an expression for the binary cluster integral with isotropic preaveraging of end group effects,[16]

$$-\frac{1}{2}\langle \beta \rangle = \frac{\pi}{4}\left[L^2 D^{\text{eff}} \rho + \frac{L^2}{\kappa}\eta + 4L\bar{D}_{\text{eff}}^2 \left(1 - \frac{4\Delta}{\pi \bar{D}_{\text{eff}}}\right) + \frac{8}{3}\bar{D}_{\text{eff}}^3 \left[1 - \frac{3\pi\Delta}{2\bar{D}_{\text{eff}}} + 3\left(\frac{\Delta}{\bar{D}_{\text{eff}}}\right)^2\right]\right] \tag{3}$$

with

$$\Delta = [(2 \ln 2)\bar{D}_{\text{eff}}/\kappa - (\ln 2)^2/\kappa^2]^{1/2} \tag{4}$$

and effective diameters

$$D^{\text{eff}} = D_0 + \kappa^{-1}(\ln A' + \gamma + \ln 2 - \tfrac{1}{2}) \tag{5}$$

$$\bar{D}_{\text{eff}} = D_0 + \kappa^{-1}(\ln A' + \gamma - \ln 2 + 1) \tag{6}$$

Here, γ denotes Euler's constant and $A' = Ae^{-\kappa D_0}$. The parameters ρ and η are proportional to the orientational pair excluded volume. For the isotropic phase these parameters take the values $\rho = 1$ and $\eta = 0$, whereas in the liquid crystalline phase they depend on the orientation distribution parameter α_D.[8,15] For the orientation entropy σ_E we use DuPré and Yang's modification of Odijk's expression, so as to agree with Khokhlov and Semenov's asymptotic limits of very flexible and very stiff wormlike chains,[17–19]

$$\sigma_E = \ln \alpha_D - 1 + \pi e^{-\alpha_D} + \frac{1}{6}(\alpha_D - 1)N_p + \frac{5}{12}\ln\left(\cosh\left(\frac{1}{5}(\alpha_D - 1)N_p\right)\right) \quad (7)$$

Here, σ_E has an explicit contour length dependence expressed as the number N_p of persistence length units. For the present DNA fragments N_p is of order unity. In the anisotropic phase the orientation parameter α_D follows from minimization of the free energy $\partial\Delta F/\partial\alpha_D = 0$. Phase boundaries are obtained from the coexistence equations between the anisotropic and isotropic phases $\mu_i = \mu_a$ and $\Pi_i = \Pi_a$, with osmotic pressure $\Pi = -(\partial\Delta F/\partial V)_{T,N,\mu_0}$ and chemical potential $\mu = -(\partial\Delta F/\partial N)_{T,V,\mu_0}$.

As will be shown below, the virial expansion of the hard core contribution has to be carried to higher order. For this purpose, the hard core reference part of the excluded volume [i.e., Eqs. (3–6) with zero screening length] is replaced by the relevant expressions given by Cotter's scaled particle theory or Lee's model. The electrostatic contribution is treated as a thermodynamic perturbation in the second virial approximation. For an extensive description of scaled particle theory in the context of liquid crystal formation of rodlike polymers the reader is referred to review papers by Sato and Teramoto,[13,16] and for the generalisation of the Carnahan–Starling equation Refs. 11 and 12 may be consulted.

EXPERIMENTAL

DNA fragments were obtained by micrococcal nuclease digestion of calf thymus chromatin.[20] Hydrolysation with proteinase K followed by repeated phenol extractions was employed to remove residual protein. The differential molecular weight distribution was monitored by size exclusion chromatography (SEC) with light scattering detection and a typical example is displayed in the top panel of Figure 1.[21] The advantage of the isolation procedure is that it yields a large quantity of mononucleosomal DNA, but a typical batch contains approximately 25% lower and higher molecular weight material. Further SEC fractionation (of two different batches) resulted in three relatively monodisperse eluent fractions FI–III. Their differential molecular weight distributions are displayed in the bottom panel of Figure 1. The average molecular weights, polydispersity characteristics, and weight average contour lengths are collected in Table I. Eluents FI and FII contain mononucleosomal DNA with a small difference in average molecular weight. Fraction FIII contains incompletely digested DNA, but with a relatively narrow molecular weight distribution centered about twice the mononucleosomal value. The ratios of the optical absorbencies $A_{260}/A_{280} = 1.91$ and $A_{260}/A_{270} = 1.21$ show the material is essentially free of protein and phenol, respectively.[22] DNA with tetramethylammonium (TMA^+) or Cs^+ counterions was prepared by flowing a Na-DNA solution (fraction FI) through a cation exchange resin (Biorad AG 50W X2). The residual Na content in Cs-DNA and TMA-DNA (without salt) was determined by atomic absorbance spectroscopy and amounts 0.6 and 0.2%, respectively. The hypochromic effect at 260 nm confirmed the integrity of the double helix. It was checked with SEC that the counterion conversion procedure did not induce DNA degradation.

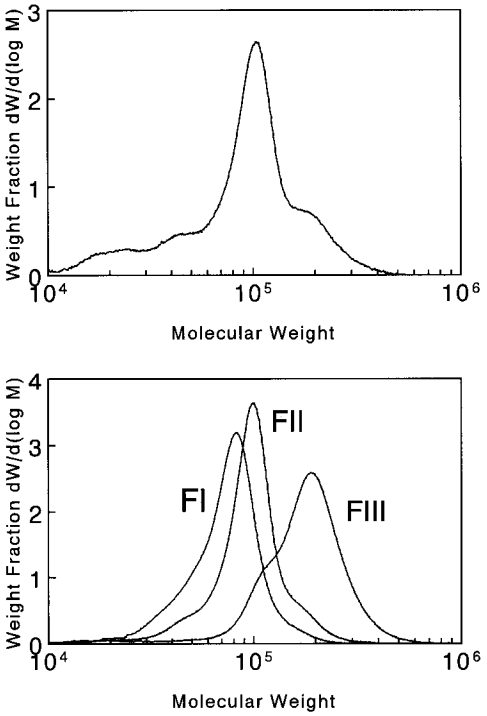

FIGURE 1 NA-DNA differential molecular weight distribution. Top panel: original batch after isolation and purification procedure. Bottom panel: eluents FI–III obtained by SEC fractionation. The molecular weight characteristics are collected in Table I.

Samples were prepared by dissolving freeze-dried DNA in pure water or NaCl, CsCl, or TMACl salt solutions. The DNA concentration was determined by weight and checked with uv spectroscopy at 260 nm. The samples were steplike diluted with pure water or the relevant salt solutions and allowed to equilibrate for 3 days to 2 weeks for the more viscous samples. After each dilution step a droplet was deposited and sealed between a microscope slide and coverslip and observed through crossed polarizers with a Leica DMR microscope with 40× and 100× objectives at ambient temperature. The hexagonal

Table I Na-DNA Average Molecular Weight M_w, Polydispersity M_w/M_n, and Weight Average Contour Length L of SEC Eluents

Fraction	M_w	M_w/M_n	L (nm)
FI	81,000	1.17	42
FII	104,000	1.14	54
FIII	202,000	1.20	104

phase appears opaque under visual inspection and exhibits the characteristic fanlike shapes under microscopic observation. The cholesteric phase is iridescent and displays fingerprintlike textures.[2] The appearance of the isotropic phase is most conveniently detected by the emergence of a isotropically narrowed ^{31}P magnetic resonance.[4] The nmr experiments were done with a Bruker AM 200 spectrometer at a ^{31}P resonance frequency of 109 MHZ and a sweep width of 100 kHz. The samples were equilibrated at least for one hour within the magnet at 298 K before spectra were taken. The C-I phase boundary concentrations were also determined from phase separation experiments.[6,7] Biphasic samples were prepared and phase separation took place over periods from 3 days to 2 weeks for samples with low amounts of added salt. Within the coexisting phases the DNA concentrations were determined by uv spectroscopy. Long-term stability, reproducibility, and agreement between phase separation and steplike dilution experiments showed that the reported results refer to samples in chemical equilibrium.

RESULTS AND DISCUSSION

Phase Boundaries

Both phase transitions are first order with relatively small differences in DNA concentration in the coexisting phases. The investigated samples were always at chemical equilibrium and there are no spatial concentration gradients. The critical volume fractions representing the appearance of the cholesteric phase and disappearance of the isotropic phase are denoted by ϕ_i and ϕ_a, respectively. Analogously, the volume fractions representing the appearance of the hexagonal phase and disappearance of the cholesteric phase are denoted by ϕ_c and ϕ_h. To allow direct comparison between solutions with different counterions, these volume fractions refer to DNA only. Boundary concentrations in mole of nucleotides/L can be obtained by dividing the volume fractions with the partial molal nucleotide volume $V_m = 172$ cm^3/mole.

The volume fractions ϕ_i and ϕ_a of fraction FII Na-DNA have been obtained from phase separation experiments and are displayed in Figure 2 vs added NaCl concentration. For fraction FI ($L = 42$ nm) Na-, Cs-, and TMA-DNA in NaCl, CsCl, or TMACl, respectively, we obtained ϕ_i and ϕ_a from phase separation as well as dilution experiments under parallel polarization microscopy and/or ^{31}P-nmr. For fraction FIII ($L = 104$ nm) the boundaries were obtained from dilution experiments only. Both experimental methods yielded similar results with a nonsystematic variation of order the reproducibility 3%. The average values are displayed in Figure 3, including the elsewhere reported critical volume fractions pertaining to the hexagonal-cholesteric phase transition (ϕ_c and ϕ_h). The critical boundary concentrations for Na-DNA/NaCl and Cs-DNA/CsCl are similar. When the cations are replaced by the more bulky TMA^+, a significant decrease in critical volume fractions is observed. Finally, Figure 4 displays the weight average contour length dependence of ϕ_i and ϕ_a of Na-DNA in 0.25M NaCl.

For 50 nm fragments, Rill and co-workers obtained ϕ_i and ϕ_a by ^{31}P-nmr and polarization microscopy in the supporting electrolyte range 0.01–1M NaCl ($T = 293$ K).[4] In this range, the critical volume fractions representing the appearance of the anisotropic phase ϕ_i vary from 0.067 (130 mg/mL) to 0.088 (170 mg/mL). Under the same conditions,

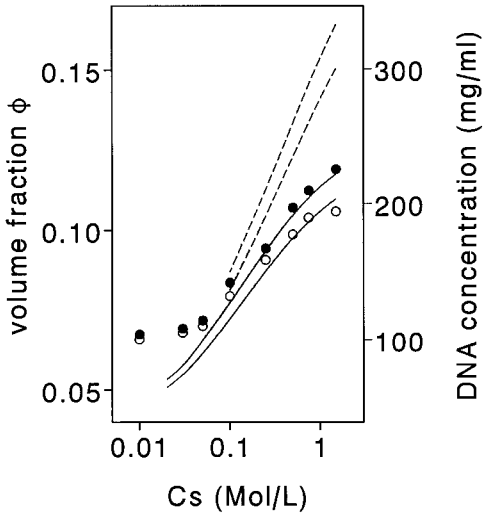

FIGURE 2 Isotropic–cholesteric phase boundary volume fractions ϕ_i (○) and ϕ_a (●) of FII Na-DNA vs NaCl concentration C_s. The right scale denotes the phase boundaries in units mg/mL. The solid curves are calculated with scaled particle or Lee's description for hard core effects and electrostatic interactions in the second virial approximation. The dashed curves are based on hard core and electrostatic interactions in the second virial approximation.

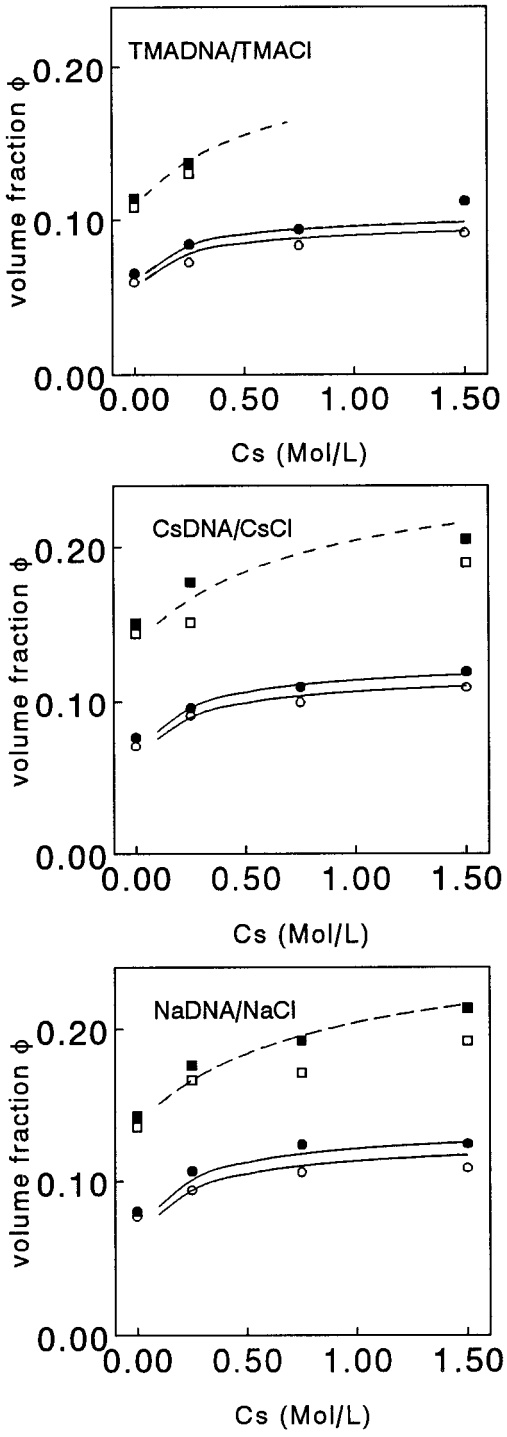

FIGURE 3 Critical volume fractions ϕ_i (○), ϕ_a (●), ϕ_c (□), and ϕ_h (■) pertaining to the isotropic–cholesteric and cholesteric–hexagonal transition, respectively, of FI DNA vs added salt concentration C_s. The solid curves are calculated as in Figure 2. The dashed curves represent the ionic strength dependence of the hexagonal melting side with Lindemann criterion $C_L = 0.098 \pm 0.003$.[5]

they reported a rather broad biphasic region with a modest ionic strength variation of ϕ_a separating the biphasic from the fully liquid crystalline solution between 0.135 (260 mg/mL) and 0.140 (270 mg/mL). Our ϕ_i results show similar behavior, although at high ionic strength the anisotropic phase appears at somewhat higher DNA volume fraction. For extremely long DNA (8 kilobases) in 0.1*M* NaCl, Merchant and Rill also reported an unexpected broadening of the biphasic region with $\phi_i = 0.007$ (13 mg/mL) and $\phi_a = 0.035$ (67 mg/mL).[23] In more recent work the same authors reported the phase boundaries as function of contour length ranging from 50 to 2700 nm in 0.1*M* NaCl.[24] For a $L = 114$ nm fragment they reported $\phi_i = 0.025$ (48 mg/mL) and $\phi_a = 0.072$ (138 mg/mL), whereas we obtained for $L = 104$ nm in 0.25*M* NaCl $\phi_i = 0.072$ (139 mg/mL) and $\phi_a = 0.077$ (149 mg/mL). Merchant and Rill tentatively explained the broadening of the biphasic regime and low ϕ_i values of fragments with longer contour lengths ($\gtrsim$114 nm) to the existence of local sequence-dependent variations in DNA flexibility and/or weakly attractive interactions. In contrast to the observations by Rill and co-workers, we observe in the contour length range 42–104 nm a relatively narrow biphasic region with a strong ionic strength dependence of both ϕ_i and ϕ_a. We did not observe precholesteric structures at low ionic strength (which have recently been marked regular cholesteric).[2]

Hexagonal–Cholesteric Transition

The hexagonal–cholesteric phase transition is discussed in another publication.[5] It was found that the transition follows the Lindemann rule, i.e., the hexagonal lattice melts when the fluctuations in transverse order exceed a certain fraction of the interaxial spacing. The spacings R were derived from ϕ_h and the fluctuations were estimated with Odijk's theory of semiflexible wormlike polyelectrolytes confined in a hexagonal lattice.[25,26] The gist of this theory is that the electrostatic interactions are *exponentially* renormalized by a large factor $\exp(\kappa^2 u^2/2)$, because the undulation amplitude u is of order the electrostatic screening length κ^{-1}. The Lindemann ratio $C_L = u/R$ was found to be constant with average value $C_L = 0.098 \pm 0.003$. The dashed lines in Figure 3 are calculated with this Lindemann ratio and bare diameter $D_0 = 2.1$ nm for Na- and Cs- and 2.3 nm for TMA-DNA. Undulation theory with the Lindemann criterion describes the ionic strength dependence of the hexagonal side of the melting transition satisfactorily. Un-

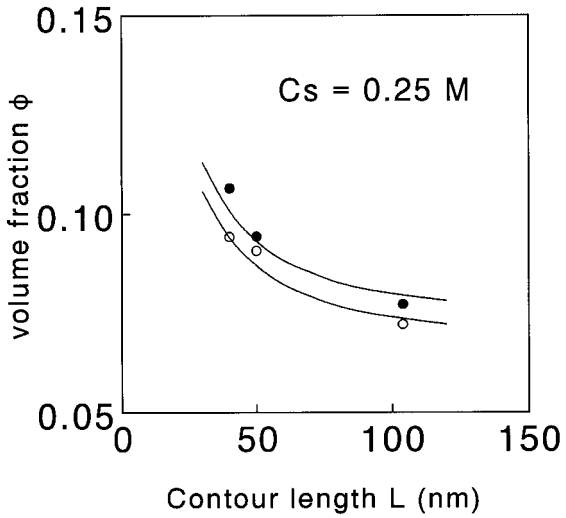

FIGURE 4 Weight average contour length dependence of isotropic–cholesteric phase boundary volume fractions ϕ_i (○) and ϕ_a (●) of Na-DNA in 0.25*M* NaCl. The solid curves are calculated as in Figure 2.

fortunately, for the cholesteric side ϕ_c no theory is available.

Cholesteric–Isotropic Transition

The C-I boundary concentrations can be calculated from the coexistence equations, which are derived from the solution free energy including orientation entropy and excluded volume effects.[8,9] For the orientation entropy we use DuPré and Yang's modification of Odijk's expression, so as to agree with Khokhlov and Semenov's asymptotic limits of very flexible and very stiff wormlike chains.[17–19] The virial terms are calculated with the assumption that the intermolecular interactions are a sum of hard core and electrostatic interactions. With the wormlike chain as reference system, the electrostatic contribution to the free energy is evaluated as a thermodynamic perturbation in the second virial approximation.[16] The hard core contribution has either been evaluated in the second virial approximation or with two approximate methods to include higher order terms: Cotter's scaled particle theory and Lee's generalization of the Carnahan–Starling equation of state for hard spheres.[10,11] For the present M_w/M_n ratios polydispersity effects on the boundary concentrations are expected to be modest and have been neglected.[24]

The electrostatic potential is obtained from the linearized version of the Poisson–Boltzmann equation for cylindrical polyelectrolytes with excess salt (Debye–Hückel approximation).[14,15] DNA counterion screening cannot be neglected and has been estimated with the condensation concept.[25] Donnan salt partitioning between coexisting phases has been taken into account according to Ref. 7. These effects are negligibly small due to small differences in DNA concentration and/or high added salt concentrations (this is also indicated by the similarity of the phase separation and dilution results for fraction F1). The potential depends on the distance of closest approach of the small ions to the DNA *z* axis. Different counterions have different distances of closest approach, due to differences in size and/or hydration properties. These effects are taken into account by optimizing the bare DNA diameter D_0. For short fragments, end effects are important and have been isotropically preaveraged.[28]

The dashed curves in Figure 2 represent the theoretical ϕ_i and ϕ_a calculated with both the hard core and electrostatic interactions in the second virial approximation. Second virial theory overestimates the boundaries at higher salt concentrations and predicts a too steep added salt dependence. It is clear that the virial expansion has to be carried to higher order due to the relatively small DNA aspect ratio. The solid curves in Figures 2–4 are calculated with scaled particle or Lee's description of hard core effects and electrostatic interactions in the second virial approximation. These approximate methods improve significantly over the second virial expansion and reproduce the fragment length and ionic strength dependence at sufficiently high salt concentrations. In the scaled particle procedure the bare diameter D_0 was set to 1.9, 2.0, and 2.3 nm for Na-, Cs-, and TMA-DNA, respectively. In case of Lee's description, these values have to be augmented by 0.1 nm for similar results. The bare diameters are in reasonable agreement with the DNA outer diameter 2 nm. As displayed in Figure 3, the cation size effect on the critical volume fractions can satisfactorily be taken into account by a small increase in D_0.

The experimental data deviate from the theoretical predictions when the added salt concentration drops below, say, 0.1*M* (see Figure 2). In this regime, electrostatic screening originates progressively from DNA counterions. An uncondensed counterion fraction 0.24 has been taken into account,[28] but for these dense systems this figure is probably underrated. The double layer is effectively more compressed, which results in a decrease in electrostatic excluded volume and an upward deviation of the boundary concentrations. As displayed in Figure 4, the theory reproduces the weight average fragment length dependence in 0.25*M* NaCl. At this

supporting electrolyte concentration, effects of DNA counterion screening are minor. A relatively strong length dependence is observed, in accordance with the fact that the contour lengths are of order the persistence length (50 nm). It should be noted that the contour length dependence of the critical boundaries results from a subtle interplay of excluded volume effects and orientation entropy. The theory predicts a leveling off at approximately twice the persistence length, in accordance with our observations for fragments with twice the mononucleosomal length.

CONCLUSIONS

We obtained the critical boundary concentrations of anisotropic phase formation in short fragment DNA solutions as function of supporting electrolyte concentration, counterion variety, and DNA contour length. Our results differ from critical concentrations published by Rill and co-workers, since they do not confirm the unexpected broadening of the biphasic region and low value of ϕ_i for the fragment with contour length being twice the mononucleosomal value.[4,23,24] Polydispersity effects are expected to broaden the biphasic region and our slightly worse M_w/M_n ratios cannot account for this discrepancy. The phase behavior is in accordance with theory incorporating the effects of chain flexibility and charge. At sufficiently high salt concentrations the agreement is almost quantitative, but for consistency higher order electrostatic terms should also be incorporated. Furthermore, the approximate methods for the evaluation of the hard core reference system need theoretical justification. At a low amount of added salt, deviations are observed. Of course, these deviations can be attributed to deficiencies in the theory, but a more obvious explanation can be found in screening effects by counterions originating from DNA. The counterion species dependence can satisfactorily be interpreted by setting a bare DNA diameter in accordance with the small ion size and/or hydration properties. Finally, the contour length dependence agrees with a DNA persistence length 50 nm and does not comply with variations in DNA flexibility.

JRC van der M. thanks T. Odijk for stimulating discussions.

REFERENCES

1. Robinson, C. (1961) *Tetrahedron* **13,** 219–234.
2. Livolant, F. & Leforestier, A. (1996) *Prog. Polym. Sci.* **21,** 1115–1164.
3. Reich, Z., Wachtel, E. J. & Minsky, A. (1994) *Science* **264,** 1460–1463.
4. Rill, R. L., Strzelecka, T. E., Davidson, M. W. & Van Winkle, D. H. (1991) *Phys. A* **176,** 87–116.
5. Kassapidou, K. & van der Maarel, J. R. C., *Eur. Phys. J. B,* in press.
6. Fraden, S., Maret, G., Caspar, D. L. D. & Meyer, R. B. (1989) *Phys. Rev. Lett.* **63,** 2068–2071.
7. Sato, T., Kakihara, T. & Teramoto, A. (1990) *Polymer* **31,** 824–828.
8. Onsager, L. (1949) *Ann. NY Acad. Sci.* **51,** 627–659.
9. Odijk, T. (1986) *Macromolecules* **19,** 2313–2328.
10. Cotter, M. A. (1977) *J. Chem. Phys.* **66,** 1098–1106.
11. Lee, S.-D. (1987) *J. Chem. Phys.* **87,** 4972–4974.
12. Hentschke, R. (1990) *Macromolecules* **23,** 1192–1196.
13. Sato, T. & Teramoto, A. (1996) *Adv. Polym. Sci.* **126,** 85–161.
14. Brenner, S. & Parsegian, V. A. (1974) *Biophys. J.* **14,** 327–334.
15. Stroobants, A., Lekkerkerker, H. N. W. & Odijk, T. (1986) *Macromolecules* **19,** 2232–2238.
16. Sato, T. & Teramoto, A. (1991) *Phys. A* **176,** 72–86.
17. DuPré, D. B. & Yang, S. (1991) *J. Chem. Phys.* **94,** 7466–7477.
18. Khokhlov, A. R. & Semenov, A. N. (1981) *Phys. A* **108,** 546–556.
19. Khokhlov, A. R. & Semenov, A. N. (1982) *Phys. A* **112,** 605–614.
20. Wang, L., Ferrari, M. & Bloomfield, V. A. (1990) *BioTechniques* **9,** 24–27.
21. Nicolai, T., van Dijk, L., van Dijk, J. A. P. P. & Smit, J. A. M. (1987) *J. Chromatogr.* **389,** 286–292.
22. Liebe, D. C. & Stuehr, J. E. (1972) *Biopolymers* **11,** 167–184.
23. Merchant, K. & Rill, R. L. (1994) *Macromolecules* **27,** 2365–2370.
24. Merchant, K. & Rill, R. L. (1997) *Biophys. J.* **73,** 3154–3163.
25. Odijk, T. (1993) *Biophys. Chem.* **46,** 69–75.
26. Odijk, T. (1993) *Europhys. Lett.* **24,** 177–182.
27. Manning, G. S. (1969) *J. Chem. Phys.* **51,** 924–933.
28. Odijk, T. (1990) *J. Chem. Phys.* **93,** 5172–5176.